Is there a continuous Subtropical Front south of Africa?

Guillaume Dencausse,[1,2] Michel Arhan,[1] and Sabrina Speich[1]

[1] A 14.3 year series of weekly absolute sea surface height (SSH) and associated geostrophic velocities is used for a study of the subtropical-to-subantarctic frontal system in the region south of Africa. Detecting the fronts from surface velocity maxima confirms a two-stepped transition in both the southeastern Atlantic Ocean (the Northern and Southern Subtropical fronts (NSTF, SSTF)) and southwestern Indian Ocean (the Agulhas Front and SSTF), as proposed previously from hydrographic data. An additional front associated with westward flow north of the NSTF is indicative of a partial eastern closure of the South Atlantic subtropical gyre between 11°E and 17.5°E. The role of northwestward propagating Agulhas rings in connecting the two fronts explains the varying location. The SSTF, which marks the southern limit of subtropical waters, is found continuous from the Atlantic to the Indian Ocean in the time-averaged SSH field. In the weekly fields, however, the velocity maximum criterion defining the front is often met at the southern flanks of Agulhas rings or Agulhas eddies at 12°E–23°E, indicating front disruptions. Such discontinuities suggest that no South Atlantic Central Water is directly advected into the Indian Ocean. Instead, the eastward limb of the Indo-Atlantic "super gyre" encompassing the subtropical gyres of both oceans would rest, at these longitudes, on diffusive processes at the upper levels, and possibly be enhanced at depth. A schematic diagram of the fronts and their relations to Agulhas rings and eddies is proposed.

Citation: Dencausse, G., M. Arhan, and S. Speich (2011), Is there a continuous Subtropical Front south of Africa?, *J. Geophys. Res.*, *116*, C02027, doi:10.1029/2010JC006587.

1. Introduction

[2] The basin-wide subtropical gyres of the South-Atlantic and South-Indian oceans are bounded southward at about the location of the zero wind stress curl, a line which, on average, runs 10° of latitude south of the southern tip of South Africa [e.g., *Peterson and Stramma*, 1991]. This leaves room for a partial connection of the two gyres, and results in the formation of a so-called super gyre encompassing the anticyclonic circulations of both oceans [*de Ruijter et al.*, 1999]. The dynamical factors influencing the degree of connection between the two gyres have been studied in the 1980s, using numerical models of increasing complexity [*de Ruijter*, 1982; *de Ruijter and Boudra*, 1985; *Boudra and de Ruijter*, 1986; *Boudra and Chassignet*, 1988; *Chassignet and Boudra*, 1988], and *Gordon et al.* [1992] from an analysis of hydrographic and tracer data, proposed a schematic representation of the large-scale circulation also exhibiting the super gyre, with interoceanic exchanges south of Africa in both directions, and in both thermocline (warmer than 9°C) and intermediate layers.

[3] Numerous studies of the northern (westward) limb of the interoceanic connection have led to a good description and understanding of its major contributing processes, namely, the pulse-like behavior of the Agulhas Current retroflection, and the related shedding of northwestward propagating Agulhas rings (see *de Ruijter et al.* [1999] and *Lutjeharms* [2006] for reviews of these studies). In comparison, the southern (eastward) limb of the interoceanic connection remains poorly described. If there be a transfer of South Atlantic Central Water into the Indian Ocean, this should occur as an extension of the South Atlantic Current (SAC) described by *Stramma and Peterson* [1990], and along the Subtropical Front (STF; formerly named Subtropical Convergence [*Deacon*, 1982]), which marks the southern limit of upper subtropical waters (or Central Waters) and is generally represented as a continuous feature between the two oceans.

[4] Using sea surface temperature sections located east of ~10°E, *Lutjeharms and Valentine* [1984] found a STF generally located south of 40°S. From a set of expendable bathythermograph data spanning a wider longitudinal range (~10°W–40°E), *Lutjeharms* [1985] located the STF on average at 41°S, yet noted a highly variable frontal position directly south of South Africa. Circumpolar studies of the Southern Ocean fronts, either using sea surface hydrographic properties [*Deacon*, 1982] or full depth hydrographic data [*Orsi et al.*, 1995; *Belkin and Gordon*, 1996],

[1]Laboratoire de Physique des Océans, CNRS/IFREMER/IRD/UBO, Plouzane, France.
[2]Now at Laboratoire d'Etudes en Géophysique et Océanographie Spatiale, LEGOS/OMP, Toulouse, France.
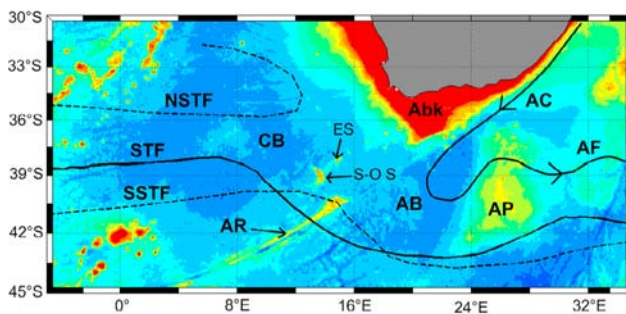
Figure 1. Map of the studied area showing the tracks of the climatologic Subtropical Front of *Orsi et al.* [1995] (STF) and Subtropical Front branches of *Belkin and Gordon* [1996] (NSTF, SSTF). The paths of the Agulhas Current (AC) and Agulhas Front (AF) are represented schematically after *Lutjeharms and Van Ballegooyen* [1988]. The main bathymetric features are indicated: Cape Basin (CB), Agulhas Basin (AB), Agulhas Bank (Abk), Agulhas Plateau (AP), Agulhas Ridge (AR), Erica Seamount (ES), and Schmitt-Ott Seamount (S-OS).

also suggest that a subtropical to subantarctic frontal transition exists continuously from the Atlantic to the Indian Ocean. A recent study of the Southern Ocean fronts by *Sokolov and Rintoul* [2009], however, contains indications that the STF continuity south of Africa should perhaps not be taken for granted. The authors detected the fronts using the gradients of altimetry-derived sea surface height (SSH). These gradients show rather patchy distributions, but *Sokolov and Rintoul* [2009] noted that their maxima in the Antarctic Circumpolar Current (ACC) are consistently aligned along particular SSH values, an indication of circumpolar continuous paths. This does not hold north of the ACC and particularly south of Africa, however, a sign that the fronts in that region (including the STF) might not be continuous.

[5] A continuous STF was present in *Stramma and Peterson*'s [1990] circulation scheme, yet the authors regarded it as density compensated south of Africa, and therefore not associated with any interocean flow. With the SAC separating from the STF near the Greenwich meridian to join in the northward flowing Benguela Current along the African coast, their representation of the currents favored the eastern closure of the South Atlantic subtropical gyre, at the expense of water transfer to the Indian Ocean. The solution proposed by *Gordon et al.* [1992] was more equilibrated, with about 50% of the SAC thermocline water, and 70% of its intermediate water proceeding to the Indian Ocean, and the other parts turning northeastward to close the Atlantic gyre. *Belkin* [1993] and *Belkin and Gordon* [1996], using hydrographic data, finally, defended the idea of a two-branch STF (Figure 1, the Northern STF (NSTF) and the Southern STF (SSTF)), the southern one extending to the Indian Ocean, while the northern one might bend northward into the Benguela Current and close the Atlantic subtropical gyre. Such double front structure was confirmed by *Smythe-Wright et al.* [1998] from hydrographic and chemical data between 15°W and 5°E, and by

Burls and Reason [2006] using satellite microwave-derived sea surface temperature data.

[6] A transfer of Atlantic water to the Indian Ocean along the southern limb of the subtropical super gyre implies a real continuity of the STF (or SSTF) south of Africa. Such continuity has generally been accepted, as the transition from subtropical to subantarctic waters which defines the STF may be detected at any longitude from hydrographic criteria, suggesting a continuous frontal track [e.g., *Lutjeharms and Van Ballegooyen*, 1988; *Orsi et al.*, 1995]. Such a view, however, might be the result of using nonsynchronous data, as *Duncan* [1968] already pointed out after observing an eddy in the Subtropical Convergence. It seems unlikely, indeed, that a continuous STF be reconcilable with the intense mesoscale activity of the region southwest of Africa. *de Ruijter et al.* [1999] also noted that the super gyre concept might be only valuable in the mean, and emphasized that "local dynamical processes in the highly nonlinear regime around South Africa play a crucial role in inhibiting the connection between the two oceans." Several observations in this highly energetic region furthermore revealed that the hydrographic STF criteria are sometimes met at the border of propagating eddies, rather than at a classical elongated front [*Lutjeharms and Van Ballegooyen*, 1988; *Gladyshev et al.*, 2008].

[7] Like the southeast Atlantic in the frontal pattern of *Belkin and Gordon* [1996], the southwestern Indian Ocean shows a two-stepped subtropical to subantarctic transition (Figure 1). The two fronts there are the Agulhas Front (AF) associated with the Agulhas Return Current near 39°S, and the SSTF generally observed 1°–2° of latitude farther south. *Gründlingh* [1978] first differentiated the two bands of intense hydrographic gradients, and although some observations showed that they may occasionally coincide [*Lutjeharms and Valentine*, 1984], others confirmed the two-front pattern. Were the SSTF in this region just the continuation of its South Atlantic counterpart (as represented in Figure 1), its differentiation from the AF would not require any particular explanation. On the other hand, an interruption of the SSTF and associated flow south of Africa would raise the question of its reformation in the southwest Indian Ocean.

[8] The frontal patterns of Figure 1, though useful to delineate water mass domains, might be misleading if interpreted in terms of interocean flow. First, because they were determined from hydrographic criteria, and a velocity criterion relative to the frontal jet would be more suitable to the issue of water transfer. Then, because frontal tracks like those of Figure 1, deduced from sparse and nonsynoptic hydrographic sections, would fail to reveal any time or space frontal discontinuities. In this paper, we use the now available long time series (~14 years) of absolute SSH and inferred surface geostrophic velocity deduced from satellite altimetry, for a weekly determination of the subtropical-to-subantarctic frontal patterns and associated velocities at the Indo-Atlantic transition. Owing to the length of the time series, a statistical analysis of the STF discontinuities and associated flows south of Africa can be conducted. Furthermore, the amplitudes of surface velocities allow us to tell eddy borders from typical larger-scale fronts. In a previous study by the same authors [*Dencausse et al.*, 2010b], the same SSH data were analyzed for a determi-
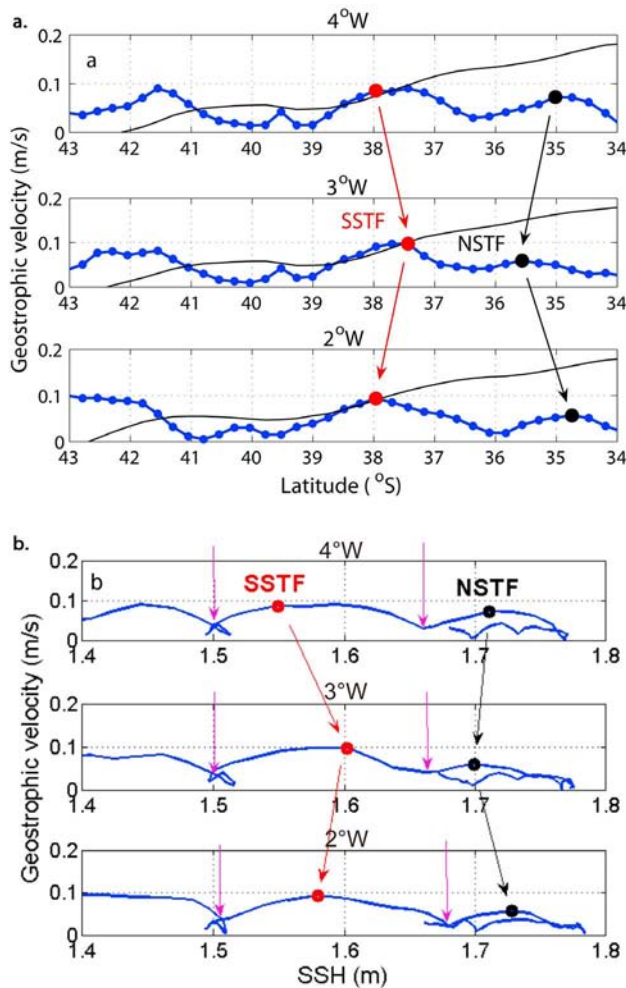
Figure 2. (a) Surface geostrophic velocities from the time-averaged SSH field as functions of latitude, at longitudes 4°W, 3°W, and 2°W. The SSH curves (black lines) are also shown, and the red and black circles mark the velocity maxima associated with the SSTF and NSTF, respectively. (b) Surface geostrophic velocities as functions of the time-averaged SSH. Magenta arrows show the limits of the SSH domains where the velocity maxima associated with the SSTF and NSTF are searched (there is no upper limit for the latter).

nation of Agulhas rings tracks and families. Results from that study are used to try and understand how Agulhas rings and other eddies interfere with the fronts, possibly causing interruptions in the SSTF, combining with the NSTF to close the South Atlantic subtropical gyre, or influencing the two-stepped frontal pattern southeast of South Africa.

[9] In section 2 of the article we present the SSH data and the method of front determination. In section 3 the frontal patterns in the time-averaged SSH field are described and shown to corroborate the double-front pattern of *Belkin and Gordon* [1996]. Section 4 shows the probability distributions of the weekly SSTF and associated velocities. The detailed longitudinal structure of the front and its relation to the mesoscale activity are examined. The NSTF and the closure of the South Atlantic subtropical gyre are discussed

in section 5, before a tentative schematic representation of fronts and eddies south of Africa in section 6.

2. Data and Methods

2.1. Data

[10] We used the absolute SSH fields and associated surface geostrophic velocities distributed by the Archiving, Validation and Interpretation of Satellite Oceanographic database (AVISO), produced by Ssalto/Duacs with support from the French Centre National d'Etudes Spatiales (http://www.aviso.oceanobs.com). The SSH fields combine a multisatellite sea surface height anomaly derived from satellite altimetry (TOPEX/POSEIDON, JASON-1, ERS) [*Le Traon et al.*, 1998; *Ducet et al.*, 2000], and a mean dynamic topography itself combining in situ data, altimetric data, and the EIGEN-GRACE 03S geoid [*Rio and Hernandez*, 2004]. Version Rio05 of this mean dynamic topography is used [*Rio et al.*, 2005]. SSH and surface velocity values are gridded with an interval of 1/3° in latitude and longitude, and are available at a weekly rate starting 14 October 1992. For this study we used the time series up to 3 January 2007, that is, 743 weeks (14.3 years), and we analyzed the fronts in the longitudinal domain 5°W–35°E.

2.2. Determination of Fronts in the Time-Averaged SSH Field

[11] As the previously proposed frontal patterns (e.g., Figure 1) were generally determined from nonsynoptic in situ data, they may be regarded as approximations of the time-averaged front tracks. First applying our front detection method to the 1992–2007 time-averaged SSH field, the previous frontal patterns could therefore be used for comparison and a coarse validation of the method. We computed the time-averaged SSH and surface geostrophic velocities, and detected the fronts of the averaged SSH field from their expected signatures as local velocity maxima.

[12] With such criterion, plotting the modulus of geostrophic velocity against SSH or latitude at any longitude of the study domain exhibits maxima which reveal the fronts. These are shown in Figure 2 for longitudes 4°W, 3°W, and 2°W. Comparing with the results of *Belkin and Gordon* [1996] (Figure 1) suggests that the two maxima observed near 38°S and 35°S in Figure 2a should be ascribed to the SSTF and NSTF, respectively. First using the plots of surface geostrophic velocities versus SSH at longitude intervals of 1°, adjacent SSH intervals where the front velocity maxima should be searched were defined between 5°W and 35°E (purple arrows in Figure 2b show the limits of these domains). Such preliminary to front detection was required to authorize longitudinally varying frontal SSH values. The limits of the SSH intervals were set at velocity minima, keeping the search intervals as large as possible while not encroaching upon the SSH range of a neighboring front. Checking the longitudinal coherence of the search intervals (as illustrated in Figure 2b) confirmed their unambiguous character. At each grid longitude (i.e., every 1/3°) the latitudes of the fronts were then determined from velocity maxima in the corresponding search intervals. We started the search from the south and, in cases when several local velocity maxima were present in the SSH interval, chose to retain the first (hence southernmost) one encountered.
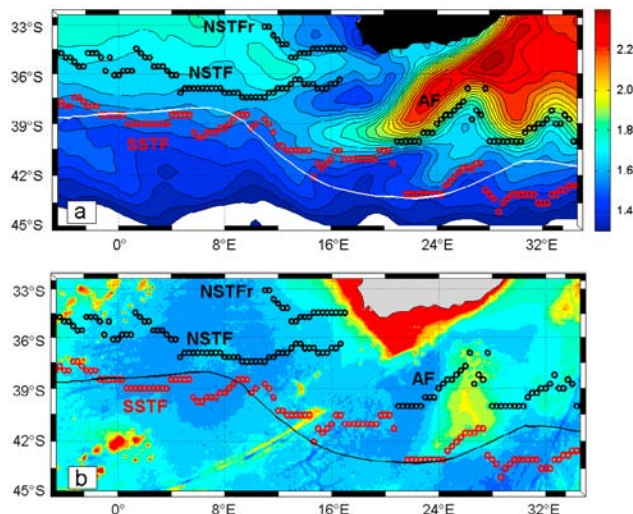
Figure 3. Front locations obtained in this study, superimposed on the (a) time-averaged SSH field and (b) bathymetry. The solid lines show the STF track of *Orsi et al.* [1995].

[13] As the fronts we are studying (SSTF, NSTF, AF) are associated with mostly eastward velocities, we furthermore only considered the velocity maxima with a positive zonal component. One exception to this was the detection of the "return" part of the NSTF (NSTFr, see below), which was carried out starting the search from the north and retaining the first (hence northernmost) velocity maximum encountered with a negative zonal component. A noteworthy consequence of these conventions is in the frontal pattern obtained in case of a local westward bend of a front track. Instead of detecting three front locations at longitudes concerned with the bend, the method only retains the southernmost one, leading to a seeming discontinuity in the front path. Finally, as a last detection criterion and in order to prevent nonrealistic shifts of the front locations, we were led to specify a reduced search latitude range at a few places where the averaged SSH is not increasing monotonously northward, as is generally the case (Figure 2).

3. Fronts of the Averaged SSH Field

[14] The fronts detected in this way are displayed in Figure 3. Their resemblance to the patterns proposed by *Belkin and Gordon* [1996] (Figure 1) led us to use the same terminology. Except for some latitudinal jumps generally due to the geographical discretization and possibly to meanders at a few locations (e.g., at 21°E), the SSTF deduced from the time-averaged SSH field appears continuous from the Atlantic to the Indian Ocean. It follows the tracks previously proposed [*Orsi et al.*, 1995; *Belkin and Gordon*, 1996], except at 15°E–20°E where it runs about 2° farther north. Its path is closer to the STF of *Orsi et al.* [1995] in the South Atlantic, but closer to the SSTF of *Belkin and Gordon* [1996] east of ~28°E. As with *Belkin and Gordon* [1996], a second front (the NSTF) was found west of ~17°E, where its search was stopped off the South African continental slope. East of 5°E, the NSTF is located at about 37°S, that is, about 1.5° south of its schematic track

in Figure 1. We looked for a possible NSTF return front as also suggested in Figure 1, and did find a westward jet just north of 35°S between 10°E and 17°E. The detection method, however, prevented us from determining the loop of the velocity jet between the NSTF and NSTFr. East of ~20°E, the detected Agulhas Return Current (AF) exhibits the well-known meander north of the Agulhas Plateau. Its track parallels that of the SSTF at a distance of ~4° of latitude, the approximate interval between the northern and southern borders of the Agulhas plateau. We note, indeed, that while the AF skirts this obstacle in the north, the averaged SSTF approximately follows the southern flank of the plateau.

3.1. The SSTF in the Averaged SSH Field

[15] In both schematic representations of the (S)STF by *Orsi et al.* [1995] and *Belkin and Gordon* [1996] (Figure 1), the front tracks bend southeastward from near 38°S–5°E to about 43°S–20°E, thus skirting the Agulhas Current retroflection to its southwest at a good distance from it. At variance with this, the altimetry-inferred SSTF, though also bending southeastward near 10°E, only reaches ~41°S, a latitude met at 13°E–15°E, near the northeastern tip of the Agulhas Ridge (Figure 3b). East of this location, the averaged SSTF seems to follow the Agulhas Return Current to about 20°E (Figure 3a), where it joins in with the nascent AF, but itself abruptly shifts to 43°S. As noted above, this apparent shift reflects the incapacity of the detection method to follow the SSH gradient meander apparent in Figure 3a. From Figure 3a alone, therefore, we cannot really tell the SSTF from the AF between 15°E and 20°E (even 23°E considering the aforementioned meander). This apparent coincidence of the two fronts on the averaged maps might result from the frequent merging of both instantaneous jets in this region, as observed by *Lutjeharms and Valentine* [1984].

[16] In Figure 4a showing the fronts surface geostrophic velocities as functions of longitude, the SSTF velocity is nearly constant, around 0.08 m/s, from 5°W to ~15°E. East of this longitude, it increases to more than 0.35 m/s at 20°E, another indication of the influence of the Agulhas Return Current on the mean SSTF at these longitudes. The SSTF velocity abruptly decreases east of 20°E, also in keeping with its separating again from the AF. The SSTF velocities in this eastern region are more variable, and more intense on average than west of 15°E.

[17] The SSH values associated with the averaged SSTF (Figure 4b) are also rather constant at about 1.55 m west of 15°E, but are more variable eastward while decreasing to 1.4 m at 35°E. Between 15°E and 20°E, the SSH variations are limited between 1.45 m and 1.65 m, that is, around the SSTF value farther west, and well below the average AF value of ~1.85 m inferred from Figure 4b. This justifies regarding the front at 15°E–20°E in the averaged SSH field as the SSTF, rather than the AF.

[18] To summarize, the SSTF identified in the averaged SSH field has a path similar to that of the hydrography-inferred fronts described in previous studies, except at longitudes 15°E–20°E (possibly 15°E–23°E), where it is found 2° farther north. This latitudinal shift, and increased frontal velocities in the same domain, reveal an influence of the AF. The questions of a possible influence of mesoscale
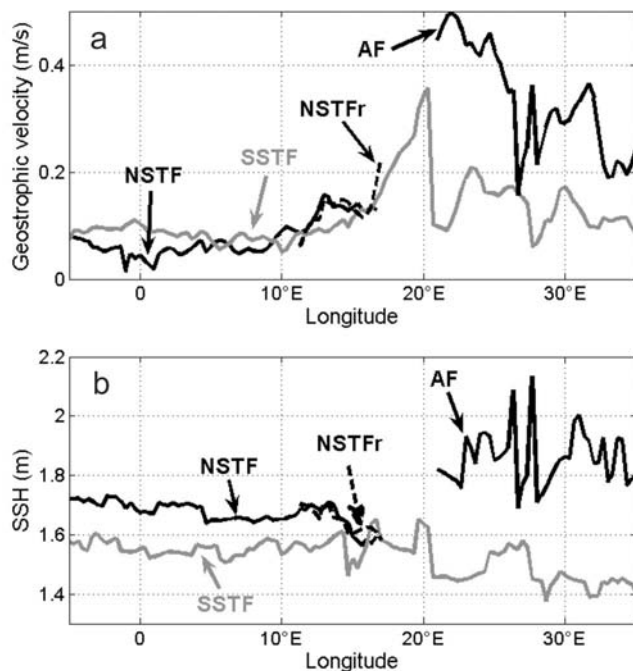
Figure 4. The (a) surface geostrophic velocities and (b) SSH associated with the averaged fronts of the subtropical-to-subantarctic transition are shown as functions of longitude.

eddies, and of possible instantaneous discontinuities, however, cannot be addressed from the averaged SSH field, and are discussed in section 4.

3.2. The NSTF and AF in the Averaged SSH Field

[19] The identification of an average front closely following the NSTF of *Belkin and Gordon* [1996] led us to look for an equatorward extent of this front, which would be a sign of partial closure of the south Atlantic subtropical gyre. Our detection of the NSTFr supports the idea of such a closure. The surface jet associated with the averaged NSTF is slightly weaker (~0.06 m/s) than the SSTF jet west of ~5°E. Like the SSTF, whose velocities increase east of ~15°E, velocities along the NSTF increase east of ~10°E, reaching 0.13 m/s between 14°E and 17°E (Figure 4a). However, unlike the SSTF velocity increase, the NSTF eastward intensification cannot be explained by an influence of the Agulhas Current or Agulhas Return Current. It should likely be associated with an averaged effect of the numerous Agulhas rings present in this region.

[20] The SSH value along the NSTF is nearly constant around 1.7 m west of 13°E, then decreases on approaching the front termination. This likely reflects an eastward gradual closure of the averaged south Atlantic subtropical gyre, apparent from an increased spacing of the averaged SSH isolines as they loop northward (Figure 3a). This broadening of the NSTF might itself be the averaged effect of time-variable southeastward extensions of the front and of the subtropical gyre. Finally, the similarity of the SSH values at the eastern ends of the NSTF and NSTFr is further indication of a connection between these two fronts and

associated jets. While this analysis of the averaged SSH field therefore confirms a partial closure of the south Atlantic subtropical gyre, it also suggests that this closure is time variable and influenced by Agulhas rings, a behavior that should be more apparent from the weekly SSH fields.

[21] Of the three frontal jets studied here, the one associated with the AF, usually referred to as the Agulhas Return Current, is the most clearly defined (Figure 3). Its velocities reach up to 0.5 m/s near 22°E (Figure 4a), yet decrease eastward to ~0.25 m/s at 35°E. As revealed from the averaged SSH distribution (Figure 3a), this decrease results from the progressive eastward closure of the inner circulation cell of the south Indian Ocean subtropical gyre, a cell which is much intensified in the southwestern part of this gyre [*Stramma and Lutjeharms*, 1997]. The associated SSH values keep a constant mean of ~1.85 m from 20°E to 35°E (Figure 4b), yet with much variation about this mean. The intense SSH gradient, and associated wide SSH range across the AF explain these variations. Owing to this wide SSH range, very different SSH values may be associated with the velocity maximum, particularly as a sampling of 1/3° is hardly sufficient to resolve such high lateral gradients.

4. The SSTF in Weekly SSH Fields

[22] The region around the Agulhas Current retroflection, and the Cape Basin, are known as areas of intense mesoscale variability [e.g., *Lutjeharms*, 2006]. Numerous anticyclonic eddies, conveying water with properties from the subtropical Indian Ocean are shed from the Agulhas Current system. A first category of these are Agulhas rings, which form at the retroflection, and propagate northwestward into the Cape Basin. Other anticyclones formed along the AF are observed in the subantarctic zone of the Antarctic Circumpolar Current [*Lutjeharms and Valentine*, 1988; *Boebel et al.*, 2003b; *Swart and Speich*, 2010] and sometimes reintegrate the subtropical domain. Numerous cyclones are also found in the region, either north of the AF [*Lutjeharms and Valentine*, 1988], or in the west-northwest of the Agulhas Current retroflection [*Lutjeharms et al.*, 2003]. The latter may originate in the subantarctic zone of the Antarctic Circumpolar Current, in the narrow oceanic strip between the African coast and the Agulhas Current, or along the South African west coast. Many of these mesoscale structures interact with the SSTF, NSTF, and AF, sometimes even originating at these fronts, and make the instantaneous tracks of the fronts far more tortuous than the time-averaged patterns of Figure 3. There have been several instances when the (S)STF, as detected from hydrographic criteria, was found at the southern border of an anticyclone [*Lutjeharms and Van Ballegooyen*, 1988; *Arhan et al.*, 1999]. This suggests that eddies might not only perturb the time-averaged SSTF track, but at places also shape up the front.

[23] In order to examine such effects, it was necessary to detect the fronts in the weekly SSH fields. This was done using the same method as for the averaged SSH field, yet with some adaptations that we describe before discussing the results.

4.1. Adaptation of the Front Detection Method to the Weekly SSH Fields

[24] Two changes were brought to the original method for the detection of the SSTF in the weekly SSH fields, and one change for the detection of the AF. For clarity, in this section we name "initial SSTF" the front obtained using the original method, and "modified SSTF" the one deduced after implementing the changes.

[25] A first method adjustment in the search of the SSTF was applied west of 19°E, the approximate average longitude of the Agulhas Current retroflection [*Lutjeharms and Van Ballegooyen*, 1988]. There, and particularly east of ~5°E, were numerous situations in which no local velocity maximum was found within the SSH intervals defined from the averaged SSH field. Examination of the weekly distributions revealed that this mainly occurred when the front was inconsistently positioned on the southern flanks of anticyclonic eddies. The positive SSH anomalies associated with such eddies may indeed result in a positioning of the velocity maximum at values higher than the upper boundary of the SSH search interval. Thus to remedy what appeared a shortcoming of the method, and to allow front detection on eddy flanks, the upper boundary of the SSH search interval was removed west of 19°E. This capacity of the modified method to detect the SSTF at eddy borders (as often occurs with hydrographic criteria) was of course essential to analyze the effects of mesoscale structures on the front continuity.

[26] The other method modification in the search of the SSTF was applied at longitudes where the AF is also present, that is, east of 19°E. Knowing that the AF and SSTF sometimes merge [*Lutjeharms and Valentine*, 1984], such occurrences should be permitted by the detection method. They were not with the original method, in which the SSH search intervals for the SSTF and AF were adjacent, hence nonoverlapping. Thus, the upper boundary of the SSH range for the SSTF was raised to 2.2 m at these longitudes, in order to have it overlap the SSH range of AF detection.

[27] The method adjustment for the AF detection consisted in starting the search north of the front, rather than south of it. This was made necessary by the occasional presence of detached anticyclones south of the AF and erroneous front detections at the rim of these structures, rather than at the real front.

[28] The front detection method thus modified was applied to each front using large latitudinal search intervals, so as to make the SSH interval the really deciding parameter. It was a priori uncertain, however, whether the SSH intervals retained for the time-averaged field would be appropriate for the weekly fields. We tested the results sensitiveness to this parameter by shifting up and down the SSH boundaries of the original method by 0.02 m. Note that for the SSTF the shift only applied to the lower boundary, as the upper SSH limit was suppressed west of 19°E, and set to the high value 2.2 m east of this longitude. Given the averaged SSH equatorward gradient in this region, SSH variations of 0.02 m correspond to averaged latitudinal shifts of about 0.2°. Variations of front latitudes lower than this value, indicative of a well-defined and well-detected front, were found for the AF, but not for the SSTF and NSTF, whose average latitudes shifted by ~0.3° and ~0.25°,

respectively. However, about 70% (for the SSTF), and 80% (for the NSTF) of the original weekly front positions were insensitive to the SSH range variations. Examining the diagrams of probability of the frontal latitudes revealed that shifting the search SSH boundaries for these two fronts caused the new search SSH range to encroach upon that of a neighboring front (the Subantarctic Front for the SSTF, and the SSTF for the NSTF), thus polluting the front detection. This examination led to the conclusion that the SSH boundaries chosen for the time-averaged field, and adapted as described above, were not influenced by the neighboring fronts, and were also an appropriate choice for the weekly fields.

4.2. Mesoscale Activity and the SSTF Continuity West of 19°E

[29] We first examine the continuity of the SSTF west of the average longitude of the Agulhas Current retroflection. Figure 5a showing the rates of SSTF detection as function of longitude obtained using the initial and modified methods, provides first information on the role of mesoscale structures. The initial SSTF rate of presence is close to 100% west of 0°E, but significantly decreases farther east to reach a pronounced minimum of 40% at 13°E. At variance with this, the modified SSTF lowest rate of presence is 87% at 10°E, and the front was detected more than 95% of the time outside the interval 5°E–15°E. The difference shows the important part played by eddies (here the southern flank of anticyclones) to define and shape up the SSTF. In order to further analyze this mesoscale contribution, we focus on the modified SSTF below, and for simplicity just name it SSTF. The latitudinal averages of the surface geostrophic velocity and SSH associated with this front are displayed, along with those of the NSTF and AF, in Figures 5b and 5c. For a more detailed analysis we also show the geographical probability of presence of the SSTF in Figure 6a and the probability densities of associated surface geostrophic velocities and SSH in Figures 6b and 6c, respectively.

[30] The geographical probability of presence of the SSTF (Figure 6a) reflects the disrupting role of eddies on the front. From 5°W to 5°E, the front confines itself to a latitudinal band of ~4° around a well-defined statistical mode at 38°S–39°S. Its latitude has a moderate standard deviation of 0.98°. Between 5°E and 19°E, on the contrary, the SSTF shows overall excursions of ~6° of latitude. There the geographical distribution does not show any pronounced mode, and the mean latitudinal standard deviation over these longitudes is 1.74°, a high value possibly indicative of a meandering regime.

[31] The role of eddies in defining the SSTF east of 5°E–10°E also stands out in the probability distributions of geostrophic velocities and SSH. West of 5°E, the front surface velocity (Figure 6b) rarely exceeds 0.3 m/s. It exhibits a well-defined mode and stable average with longitude around 0.15 m/s, comparable to values between 0.075 m/s and 0.14 m/s reported by *Whitworth and Nowlin* [1987] and *Stramma and Peterson* [1990] for the SAC east of 30°W. The mode is observed to ~12°E, but the average SSTF surface geostrophic velocity increases significantly east of ~10°E, to nearly 0.8 m/s at 19°E, and its distribution broadens drastically. At 19°E, the SSTF surface velocities range from 0.1 m/s to 1.4 m/s, values around and above
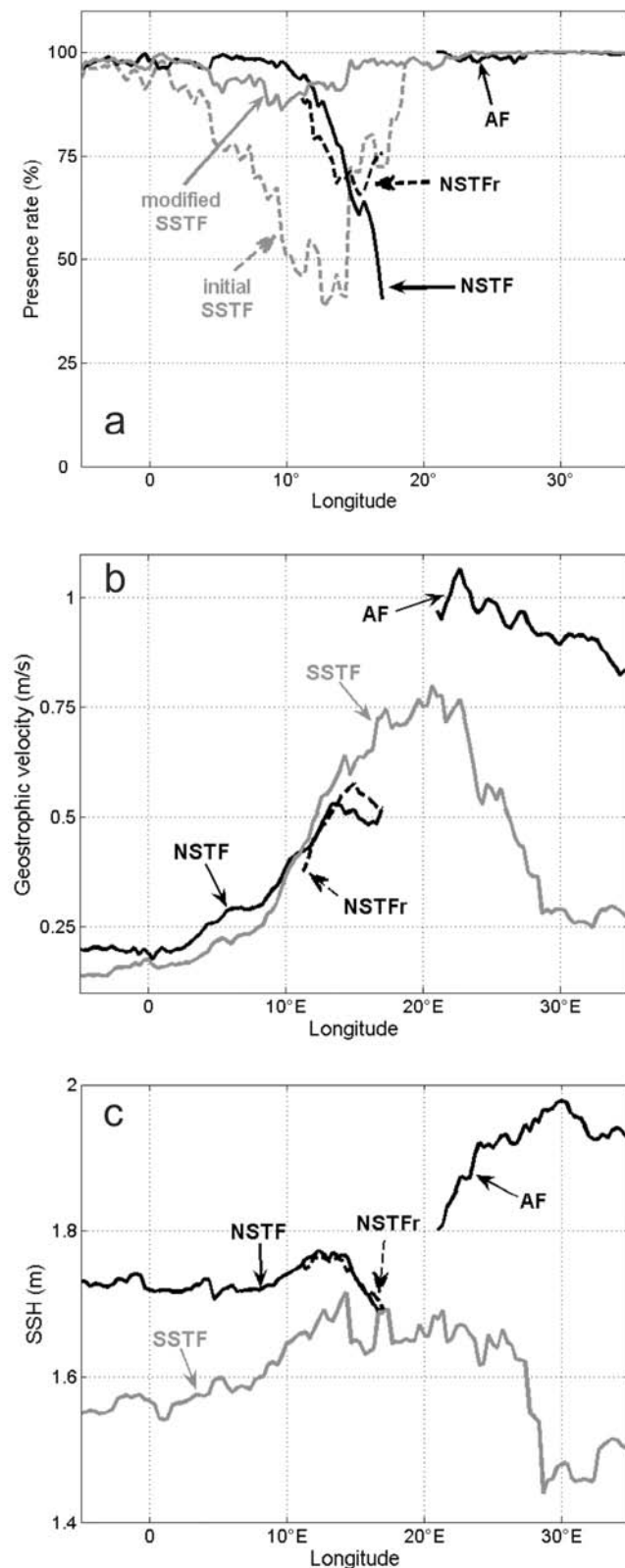
1 m/s being typical of eddies detached from the Agulhas Current retroflection.

[32] In Figure 6c, the distribution of SSH values associated with the front is also narrow (1.45 m to 1.7 m) at 5°W, with a pronounced mode at 1.55 m. Like the velocity mode, the SSH mode is found as far east as ~12°E, an indication that this is the eastern limit of the classical SAC as described by *Stramma and Peterson* [1990]. The range of frontal SSH values, however, starts to widen eastward at 3°E–5°E, and this is also the location where the averaged SSH curve separates from the modal maximum. This marks the western limit of front detections at the border of eddies, so that the transitional interval 3°E–12°E is probably where the SAC starts to merge with the eddy field. The range of frontal dynamic heights further widens eastward, with values as high as 2 m reached at 15°E. From *Dencausse et al.* [2010a], such values are only found within the loop of the Agulhas Current retroflection and in the anticyclones which detach from it at its western tip (the Agulhas rings) or from the AF [*Lutjeharms and Valentine*, 1988].

[33] From the above discussion, Figures 6a–6c corroborate the idea that while the SSTF exists as a typical elongated front west of ~12°E, it starts to be occasionally detected on the flanks of eddies detached from the Agulhas Current retroflection (Agulhas rings) east of ~5°E, and more prominently so east of ~12°E. Figure 7 showing the weekly SSH distribution on 6 May 1998, illustrates the above description. At that date, the front was well defined and relatively continuous west of ~7.5°E, east of which longitude it was disrupted by meanders and eddies. The front was actually detected at the southern flank of two Agulhas rings at 12°E and 15°E, and farther east (20°E, 24°E) at the edges of two other anticyclones likely detached from the AF.

[34] Returning to Figure 6a, we mentioned above that at longitudes 10°E–19°E where the SSTF is mostly detected at eddy rims, the probability of presence of the front showed no mode comparable in magnitude to the one observed farther west. A close examination nevertheless reveals a zonal band of most probable front locations at ~40°S, which connects to the AF farther east. In a study of Agulhas ring trajectories from the same SSH data, *Dencausse et al.* [2010b] distinguished three routes which they named northern, central, and southern, for those rings which enter the Atlantic Ocean north of the Erica Seamount (Figure 1), between the Erica Seamount and the Agulhas Ridge, and south of the Agulhas Ridge eastern tip, respectively. They observed that, between 10°E and 14°E, the STF approximately follows the southern envelope of the central route trajectories [*Dencausse et al.*, 2010b, Figure 15a]. Thus the zonal band of higher probability at ~40°S in Figure 6 most likely results from front detections at the southern side of

Figure 5. (a) Rates of presence of the fronts deduced from the weekly SSH maps, as functions of longitude. The two SSTF curves refer to the fronts obtained by the initial method (similar to the one used for the time-averaged SSH field) and the modified method (which allows for front detection at the borders of mesoscale eddies). (b) Longitudinal evolutions of the averaged surface geostrophic velocity of the different fronts. (c) Same as Figure 5b but for the averaged SSH values associated with the fronts.
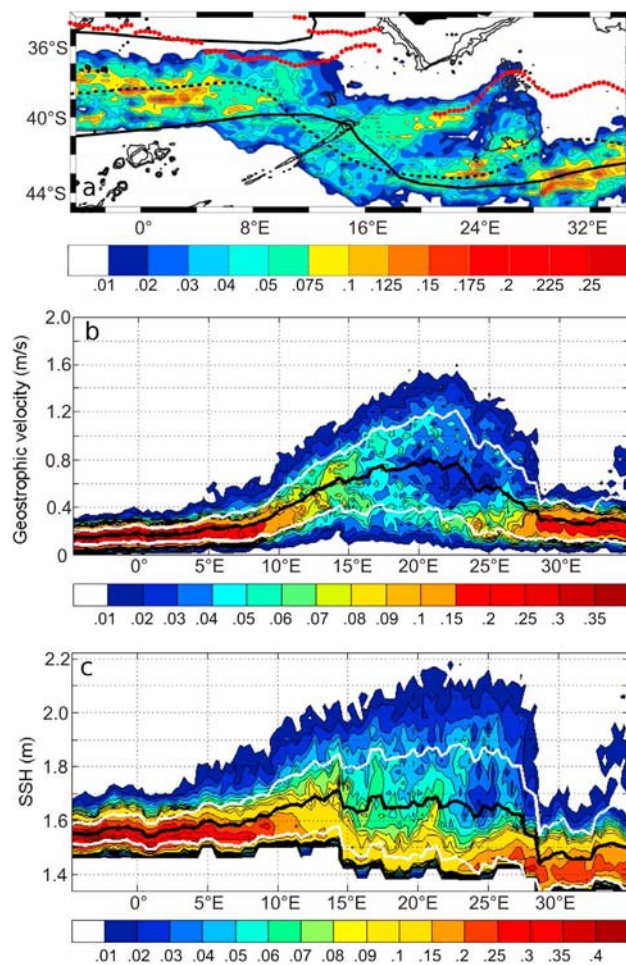
Figure 6. (a) Probability density of presence of the SSTF deduced from weekly SSH fields. In black are the climatologic fronts of *Orsi et al.* [1995] (dashed line) and *Belkin and Gordon* [1996] (solid line). Red circles show the averaged NSTF, NSTFr, and AF, also deduced from the weekly SSH fields. Bathymetric contours 500, 1000, 2000, and 3000 m are shown. (b) Probability density of surface geostrophic velocities associated with the SSTF as function of longitude, with the mean and standard deviation intervals superimposed. (c) Same as Figure 6b but for the SSH.

these rings. The fact that the rings detach from the retroflection before drifting westward further explains the statistical connection with the AF. We note that this apparent junction of the front with the AF matches the SSTF track obtained from the averaged SSH field.

[35] A secondary band of higher probability of presence in the eddy-dominated region of Figure 6a is present near 42°S, between 12°E and 17°E. Again referring to the work of *Dencausse et al.* [2010b], this most likely reflects front detections at the southern borders of Agulhas rings of their southern route, which are often observed stalling southeast of the Agulhas Ridge before crossing this obstacle northwestward. This sort of bimodal probability of presence of SSTF (see longitude 15°E) has a counterpart in the proba-

bility distribution of geostrophoc velocities (Figure 6b), which exhibits a first eastward increasing mode reaching up to ~1 m/s at 19°E, and a second one at ~0.4 m/s. The former corresponds to the 40°S geographical mode and to Agulhas rings of the central route. The latter is associated with rings of the southern route. *Dencausse et al.* [2010b] emphasized the rapid erosion of these rings as they propagate southward after their formation, a likely explanation for the lower velocities at their rims.

4.3. The SSTF East of 19°E

[36] The aforementioned bimodal character of the SSTF probability of presence is much more pronounced, and equilibrated, east of 19°E (Figure 6). Two well-defined bands of preferred SSTF locations stand out there, one identical to the AF, and the other one at ~43°S. This bimodality exists as far east as 23°E, beyond which longitude the SSTF is no longer found along the AF, but exclusively near 43°S. At 19°E–23°E the high probability of presence of the SSTF along the AF matches the observations of frequent merging of the two fronts by *Lutjeharms and Valentine* [1984]. At the same longitudes the southern maximum near 43°S follows the STF track proposed by Orsi *et al.* [1995], and deviates by less than 1° from the SSTF of *Belkin and Gordon* [1996]. An explanation for the SSTF mode at 43°S is given by *Lutjeharms and Valentine* [1988], who described several varieties of eddies detached from the AF, among which are anticyclones that may stay for several months in that region, south of the AF and north of the Subantarctic Front. The SSH distribution for 6 May 1998 in Figure 7 exhibits three such eddies, at 43°S–20°E, 41°S–24°E, and 42°S–28°E. Figure 7 shows how the SSTF detection method may position the front at the southern border of such eddies (e.g., at 20°E), or at the AF (e.g., at 22°E).

[37] This explanation for the bimodal character of the SSTF locations at 19°E–23°E is corroborated by the probability densities of the frontal geostrophic velocities (Figure 6b), which also exhibit a bipolarity that extends the one at 10°E–19°E. The core of values close to 1 m/s corresponds to a positioning of the SSTF on the AF, as such values are clearly associated with the latter front. The core of lower values, centered on 0.35 m/s, corresponds to SSTF positions around 43°S, at the border of anticyclones.

[38] The SSTF bimodality disappears at about 23°E, east of which longitude only remains the most generally recognized position around 43°S, extending the front southern core from farther west. The surface velocities in this southern core decrease eastward from 0.35 m/s at 19°E–23°E to 0.25 m/s east of 23°E. This velocity decrease, combined with the disappearance of the northern mode, suggests a decreasing role of anticyclones in defining the front path. Their effect seems to totally disappear at 28°E, where the distributions of the SSTF latitude, surface velocity and SSH (Figures 6a–6c) all significantly narrow around a unique and well-defined mode. The probability distributions there strongly resemble those associated with the SAC west of 5°E, a suggestion that the SSTF east of 23°E regains the form of a typical front with a dominant zonal orientation. There the SSTF core velocities are relatively stable around 0.25 m/s, a value higher than those of the SAC. This result matches observations of pronounced property gradients in
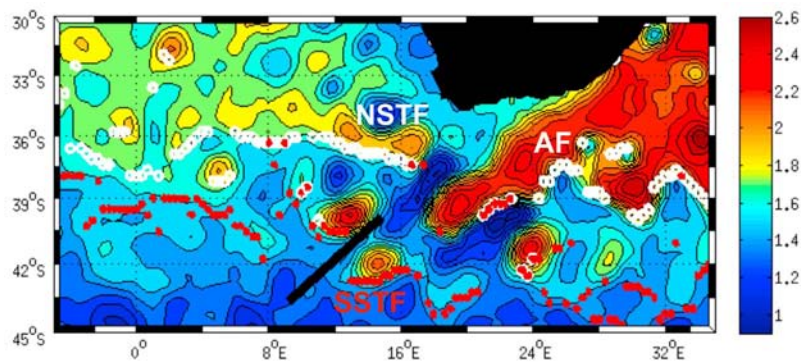
Figure 7. The fronts as detected from the SSH field of 6 May 1998. Note the coincidence of the SSTF and AF at 20°E–22°E, and several front detections at eddy borders. The thick black line segment schematizes the Agulhas Ridge.

this region by *Lutjeharms and Valentine* [1988] and *Belkin and Gordon* [1996]. Also noteworthy is the change of SSH value associated with the SSTF when passing from the Atlantic to the Indian Ocean (Figure 6c). The observed decrease from 1.55 m to 1.42 m is suggestive of an effective discontinuity of the front south of Africa.

4.4. Net Contribution of the Anticyclones and AF to the SSTF Definition

[39] The above analysis confirms the capacity of the modified SSTF detection method to locate the front at the rims of anticyclones and at the AF. We cannot state that the original detection method systematically missed front locations at eddy flanks or along the AF, because velocity maxima in such cases may occasionally be found at SSH values low enough to be within the SSH intervals defined originally. This likely concerns a minority of cases, however, so that comparing the longitude spreads (not necessarily continuous) over which each method failed to detect a front should provide a first guess of the net contribution of eddies and AF to the SSTF detection.

[40] Figure 8 (solid red curve) shows that, on average, the initial SSTF was absent over ~6° of longitude in the weekly SSH fields. There was always 2° of longitude at least over which no front was detected, and the spread with no front could reach up to 10° in some weekly fields. At variance with this, the spread with no (modified) SSTF detected does not exceed 1° in more than 50% of the weekly fields, and never exceeds 5° (dashed red curve on Figure 8). Comparing the peaks of the two SSTF curves of Figure 8 shows that this front is detected at eddy borders, or at the AF, over an accumulated spread of ~5° of longitude. This rough estimate is probably an underestimate because of occasional detections at low SSH values at eddy borders, as mentioned above. This analysis allows us to state that the classical zonally oriented SSTF present in the South Atlantic and South Indian oceans shows an average gap of about 5° of longitude south of Africa. There the surface velocity maxima used as front detectors elsewhere are also found, yet at eddy rims or at the AF, and with intensities clearly exceeding those of the SAC and of the SSTF in the south-

western Indian Ocean. These high velocities demonstrate that the latitudinal variability in this domain does not result from a meandering of the classical SSTF, nor from its positioning along eddy structures that have detached from the front. As might be expected in this region, the involved eddies are either Agulhas rings formed at the Agulhas Current retroflection, or eddies shed from the AF.

[41] While the high rate of presence of the (modified) SSTF in Figure 5a might have suggested that the front is nearly continuous from the Atlantic to the Indian oceans, the above comments on Figures 6–8 point to a radical change of flow regime south of Africa. There the classical SSTF described in previous studies leaves room for an eddy-dominated and more turbulent regime. This questions the notion of instantaneous frontal continuity. The SSTF-unrelated origin of the eddies, evident from their high velocities, discards the idea of a mere intensification of the SSTF meandering, and suggests instantaneous frontal discontinuities. While a very tortuous track of the SSTF based on SSH isolines could probably be traced from the Atlantic to the Indian oceans in each weekly field, regarding the
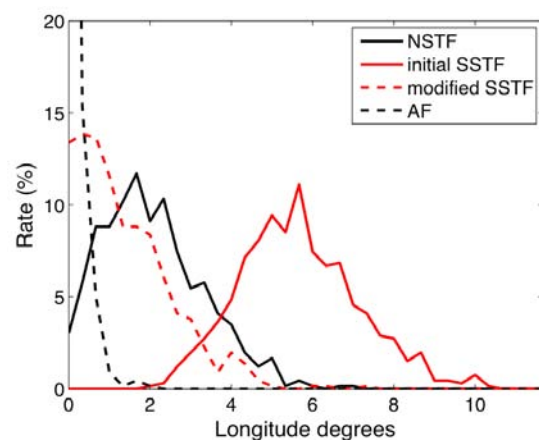
Figure 8. Rate of absence of the fronts, as function of the accumulated longitudinal range of absence.
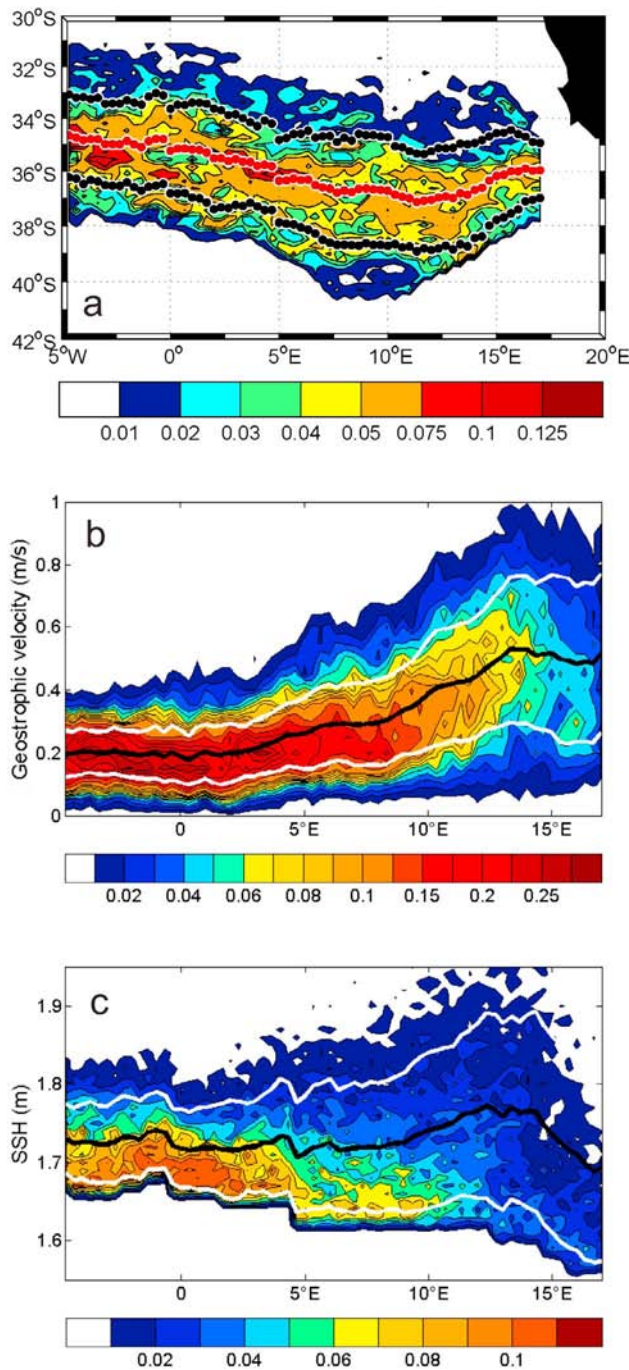
Figure 9. (a) Probability density of presence of the NSTF, with the latitudinal time-average and ±1 standard deviation intervals superimposed. (b) Density probability of surface geostrophic velocities associated with the NSTF, as function of longitude. The average curve and ±1 standard deviation curves are superimposed. (c) Same as Figure 9b but for the SSH.

instantaneous fronts as discontinuous seems nonetheless more realistic when referring to the question of frontal water transport. For the original SSTF will undoubtedly loose its identity when joining in the rims of several anticyclones

between the two oceans, and the water it conveys will likely blend in the crowd of eddies the front has to skirt.

5. The NSTF and the Closure of the South Atlantic Subtropical Gyre

[42] The search method was also modified to detect the NSTF in the weekly SSH fields, by setting the upper limit of the SSH search range to the high value 2.2 m, thus allowing front detections at eddy borders. Figure 5a shows NSTF rates of presence higher than 95 percent west of 12°E, then significantly decreasing to ~40 percent at 17°E where the search was stopped. The geographical probability of presence (Figure 9a) exhibits a clear mode at 34°S–37°S, with a slight southeastward orientation up to ~10°E, deflecting northeastward east of this longitude. West of ~10°E, the front latitudinal distributions spread over intervals of ~6°, significantly wider than the SSTF latitude ranges of ~4° west of 5°E, and likely indicative of more meandering. This widespread distribution reflects in a rather high latitudinal standard deviation of ~1.65° on average over the 5°E–17°E domain. The front surface geostrophic velocities also show a pronounced mode which is relatively stable at ~0.2 m/s west of 2°E, and increases to 0.5 m/s at 14°E. Farther east the mode strongly diminishes and the averaged velocity stays at about 0.5 m/s. While the NSTF velocities in the time-averaged fields were lower than those of the SSTF, Figure 5b shows that the reverse holds in the weekly fields, at least west of 10°E, that is, where eddies do not intervene in the SSTF definition. The difference likely results from the higher latitudinal variability of the NSTF and ensuing higher smoothing in the time-averaged field. The relatively higher instantaneous intensity of the NSTF found here somewhat contradicts the statement of *Smythe-Wright et al.* [1998], that "in general the flows associated with the SSTF are marginally higher" than those of the NSTF.

[43] The study of the NSTF in the time-averaged SSH field in section 3 suggested that this front and the NSTFr combine in a partial eastern closure of the South Atlantic subtropical gyre. There was also indication that the location of this closure near Africa was time variable. Both suggestions are corroborated by the analysis of the weekly SSH fields. East of 10°E, the NSTF bends northeastward (Figure 9a) and, although the connection to the NSTFr could not be detected by our search method, the latter front does exist in the weekly fields (Figure 6a). Moreover, its associated surface velocity and SSH relations to longitude connect to those of the NSTF at 17°E, and nearly follow the latter over the 11°E–17°E interval (Figures 5b and 5c). This further supports the idea of a permanent connection between the NSTF and NSTFr, as shown in Figure 4 of *Belkin and Gordon* [1996], and of an ensuing partial closure of the South Atlantic subtropical gyre.

[44] As mentioned in section 3, the widening of SSH isolines of the time-averaged field as they turn northward into the southeast Atlantic Ocean suggests that the longitudinal extent of the subtropical gyre varies with time. The pronounced decreases of the NSTF and NSTFr rates of presence east of ~10°E (Figure 5a) further support this idea. This spatially variable eastern termination of the gyre should be ascribed to Agulhas rings. The SSH distribution for 6 May 1998 in Figure 7, which illustrates NSTF detections
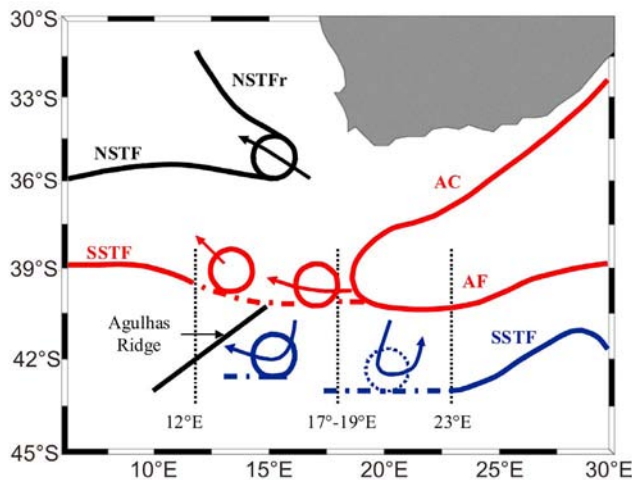
Figure 10. Schematics of the front patterns at the subtropical-to-subantarctic transition south of Africa, in relation to anticyclonic Agulhas rings (solid circles) and eddies (dashed circle). The three colors used to represent Agulhas rings are meant to distinguish between the three families (northern, central, and southern) as defined by *Dencausse et al.* [2010b].

along the southern flanks of such structures at about 36°S and 10°E–16°E, strongly suggests their determining role in supporting the NSTF east of ~10°E. The NSTF is expected to wrap around such eddies and benefit from their anticyclonic circulation to close the subtropical gyre. As the rings drift (north)westward, they modify the eastern extent of the gyre. The participation of Agulhas rings in the gyre termination is borne out by the eastward increase of the NSTF surface velocity east of ~2°E (Figures 5b and 9b). At variance with the rings effect on the SSTF SSH values, however, no clear increase of the NSTF SSH values is observed at longitudes where this front is influenced by the Agulhas rings. The SSH averaged values of the NSTF do not vary much (Figure 5c), and even decrease east of ~15°E. Figure 7 again suggests an explanation for that. At longitudes around 16°E, an area of pronounced low SSH value is present south of the anticyclonic structure supporting the NSTF. These low SSH values either signal subantarctic water which has been entrained into this region by newly formed Agulhas rings [*Lutjeharms and Van Ballegooyen*, 1988], or a cyclonic structure often present west of the Agulhas Bank and named the "lee eddy" by *Penven et al.* [2001]. This domain of lower SSH likely reduces the SSH values where a velocity maximum is found at the transition with the Agulhas rings farther north.

[45] The probability distribution of the accumulated longitudinal length over which the NSTF is not detected (Figure 8) brings further information on the front eastern extent. Most frequently, the front is not detected over a longitudinal span of 1.5° in the search interval 5°W–17°W. Given the monotonous eastward decrease of the rate of presence (Figure 5a), this gap likely represents a nearly continuous segment at the eastern end of the search domain, dictated by the position of an Agulhas ring around which the front wraps to head equatorward as the NSTFr. This would

locate the most likely eastward limit of the NSTF at about 15.5°E. Figure 8 reveals that 3 percent of the time the front was detected everywhere in the search domain, an indication that it sometimes extends slightly farther east than 17°E. Extrapolating the NSTF curve of Figure 8 to negative abscissa suggests an additional 0.5° interval, to about 17.5°E. Similarly, as the largest accumulated gap of ~6° in Figure 8 is indicative of most retracted NSTF extremities near 11°E, the variations of the front end, and of that of the NSTFr, are likely to take place between ~11°E and 17.5°E, with a most probable presence around 15.5°E.

6. Discussion

[46] When attempting to synthesize the front descriptions deduced from the weekly SSH fields, it is useful to associate them with results of *Dencausse et al.* [2010b] on Agulhas rings trajectories. As briefly reminded in section 4, three Agulhas ring families were distinguished, according to the routes taken by these structures when entering the Atlantic Ocean. Those propagating northwestward between the South African continental slope and the Erica Seamount (Figure 1), a passage devoid of major topographic obstacles, constituted the so-called northern family. Those taking the passage between the Erica Seamount and the northeastern tip of the Agulhas Ridge were named the central family, and those transiting still farther south through the Subantarctic Zone formed the southern family. *Dencausse et al.* [2010b] underlined the different obstacles the three varieties have to face when exiting the Agulhas Basin, the different water masses they go through, and the different air-sea exchanges they experience. Here we emphasize their relations to the frontal system south of Africa, and their roles regarding the questions of the SSTF continuity and eastern closure of the South Atlantic subtropical gyre. Figure 10 summarizes the main findings and suggestions.

6.1. The Closure of the South Atlantic Subtropical Gyre

[47] Starting with the issue of the gyre closure, the suggested role of Agulhas rings in connecting the NSTF to the NSTFr for a partial closure of the gyre is schematized in Figure 10. The latitude of the NSTF around 36°S (Figures 1 and 9a), that is, more than 2° north of the Erica Seamount, indicates that these Agulhas rings are from the northern route of *Dencausse et al.* [2010b]. An examination of the set of trajectories of these rings in their article [*Dencausse et al.*, 2010b, Figure 13a] reveals a westward penetration up to 10°E–12°E at 36°S, in keeping with the above conclusion that the westernmost gyre terminations are around 11°E. *Dencausse et al.* [2010b] observed that northern route rings may sometimes be found eastward right against the African continental slope, a result also corroborated by our ~17.5°E estimate for the easternmost gyre extent, a longitude which, at ~36°S, is above the 3000–4000 m isobaths at 100–130 km distances from the steep continental slope. Such occasional proximity of the gyre termination to the continental slope should be of importance for efficient exchanges at these latitudes between the ocean interior and the coastal regime. Supporting the view that Agulhas rings contribute to the southeastern closure of the South Atlantic subtropical gyre close to the continental slope is a map of dynamic topography

at the sea surface relative to 1500 dbar given by *Gordon and Bosley* [1991], which depicts such a situation. In their map, the large-scale dynamic topography contours wind around a well-defined Agulhas ring centered at ~35°S–15°E, which indeed pushes the gyre southeastern end to about 17°E.

6.2. The SSTF Continuity

[48] The issue of the SSTF continuity requires a more complex schematic representation (Figure 10) in which several longitudinal subdomains must be distinguished. The limits of the subdomains as indicated on Figure 10 and used hereafter should be regarded as indicative transitional values, as the subdomains generally overlap over a few degrees of longitude.

[49] West of 12°E, and east of 23°E, apparently continuous SSTF sections are observed, which are statistically well defined in latitude and SSH values, and associated with relatively weak geostrophic velocities of ~0.15 m/s and ~0.25 m/s in the western and eastern domains, respectively. In the Atlantic, the SSTF here determined from its velocity maximum, is located 2°–3° of latitude south of the NSTF, and should most likely be associated with the SAC of *Stramma and Peterson* [1990]. In the western Indian Ocean, our detected SSTF at ~42°S is also well distinct from the AF at ~39°S, and its location matches those previously deduced from hydrographic data [e.g., *Read and Pollard*, 1993; *Park et al.*, 2001].

[50] From 12°E to 17°E–19°E, the SSTF is mostly detected on the southern flanks of Agulhas rings from the central route of *Dencausse et al.* [2010b], at about 40°S, along a strip which connects to the AF at its eastern end. At the same longitudes, another less pronounced detection area was observed at ~42°S at the southern borders of Agulhas rings of the southern route. From 17°E–19°E to 23°E, this latitudinal bipolarity is more pronounced and more equilibrated between (1) a coincidence with the AF at 39°S–40°S already noted by *Lutjeharms* [1985] and (2) a band at about 43°S indicative of front detections at the southern edges of Agulhas eddies [*Lutjeharms and Valentine*, 1988; *Boebel et al.*, 2003b]. At 23°E the latter band connects to the more classical and continuous SSTF of the southwestern Indian Ocean. The latitudinal shift of the SSTF southern mode from ~42°S to ~43°S observed here at 17°E–19°E reminds of a comparable shift of the Subtropical Convergence at 20°E noted by *Lutjeharms and Valentine* [1984] in a study of surface thermal fronts south of Africa.

[51] As already pointed out in section 4, the finding of the front (here from velocity maxima, in other studies from hydrographic criteria) at eddy borders, and the joining of continuous front sections in the two oceans to different eddy varieties, indicate a clearly disrupted SSTF south of Africa. Such configuration suggests that the transfer of subtropical water from the Atlantic to the Indian Ocean is, at most, limited, and occurs through turbulent exchanges rather than advection.

6.3. The Question of the SSTF Formation in the Indian Ocean

[52] In the above conceptual description of the interactions between fronts and anticyclones south of Africa, the disappearance of the Atlantic SSTF at ~12°E is readily explained by its encounter with intense eddies (Agulhas rings and cyclones) and the ensuing entrainment and blending of its water by these structures. The reason why the SSTF reforms at ~23°E, east of a ~10° longitudinal interruption, remains obscure. There the SSTF marks the southern limit of a region where water properties are intermediate between those of the South Indian Central Water (found north of the AF) and those of subantarctic waters (south of the SSTF) [*Read and Pollard*, 1993; *Holliday and Read*, 1998]. The schematic view of Figure 10 may help understand how the region between the AF and SSTF east of 23°E may be occupied by water of intermediate properties, but does not help understand why a front develops at the southern border of this domain. Whether local environmental factors (such as the eddy field or local bathymetry) could explain why the jet-like flow associated with the SSTF reforms would require dedicated studies of the regional ocean dynamics. A result from *Sokolov and Rintoul* [2009] might be indicative of another explanation. Working on the ACC fronts, the authors distinguish a northern branch of the Subantarctic Front which they observe meandering around 42°S in our study region, a latitude close to that of the SSTF east of ~23°E (Figures 6a and 10). Provided that this frontal branch is itself continuous south of Africa (*Sokolov and Rintoul* [2009] regarded it as circumpolar), a change of water mass properties north of it might justify renaming it SSTF east of ~23°E.

[53] Regarding water properties, it is most likely that the region bounded by the AF and SSTF east of 23°E receives its water from the west, that is, given the absence of a continuous SSTF between 12°E and 19°E, from the domain bounded meridionally at ~36°S and ~43°S, and zonally at ~12°E and the Agulhas Current/Agulhas Return Current system. This domain approximately represents the southern half of the area which *Boebel et al.* [2003a] called the Cape Cauldron, here slightly extended southward to include the Agulhas ring southern route of *Dencausse et al.* [2010b] and the anticyclonic Agulhas eddies described by *Lutjeharms and Valentine* [1988]. It is itself fed from various sources from the Atlantic, Southern and Indian oceans. One is South Atlantic Central Water arriving from the west along the SSTF and in the band between this front and the NSTF. Another likely important source is subantarctic water, either also arriving from the west south of the SSTF, or progressing northward in between the Agulhas rings through the domain's southern boundary. Arriving from the northeast is Agulhas coastal water that has flown along the inshore side of the Agulhas Current before gathering in the lee eddy west of the Agulhas Bank and being mixed in the turbulent regime. The last important source to create the band of water with intermediate properties south of the AF is most certainly South Indian Ocean Central Water entrapped in Agulhas rings and eddies and subsequently released as these structures get eroded. Of particular importance should be the erosion of the Agulhas rings of the southern variety and of Agulhas eddies, which all migrate south to about 42°S–43°S in the subantarctic zone, the very latitude band of the SSTF farther east. These structures, that were observed to stay south of ~40°S for several months, likely release their subtropical water in the subantarctic environment, generating waters of intermediate properties which, when advected eastward in the Antarctic Circumpolar Current, might create the observed band of mixed water.

[54] Some supporting information to the diversity of water sources for the region between the AF and SSTF east of 23°E may be found in analyses of subsurface float trajectories that were carried out by *Boebel et al.* [2003a]. Figure 9h from *Boebel et al.* [2003a] study shows hindcasts of all float trajectories (at intermediate water depths) that transected a 2° width box-shaped area centered at 42°S–20°E, just west of our area of interest. Prior to crossing their test area, the floats indeed transited through the above suggested mixing region, which they nearly totally occupied along extremely tangled trajectories. Proceeding upstream, the water source locations mentioned above are recognized in Figure 9h from *Boebel et al.* [2003a], except for the Atlantic source between the NSTF and SSTF, although floats were launched in that region.

7. Conclusion

[55] The analysis of fronts as detected from velocity maxima in the time-averaged SSH field confirms the configuration proposed by *Belkin and Gordon* [1996], with a two-step transition from the subtropical to the subantarctic domain both in the Atlantic and in the southwestern Indian Ocean, and a continuous SSTF from one ocean to the other. The statistical analysis carried out on the weekly fields, however, revealed that this continuity is only apparent, and the result of time averaging. At longitudes from ~12°E to 23°E and at any given time, the SSTF criterion was rather met at the borders of anticyclones shed from the Agulhas Current retroflection or Agulhas Return Current. This led to "frontal" surface velocities and SSH values totally unlike those found farther west and farther east. It points to a situation different from that of a mere local enhancement of the front meandering, and reflects real instantaneous frontal disruptions in the above longitude interval.

[56] This conclusion questions the existence of an eastward flow of subtropical water associated with the Indo-Atlantic super gyre. If the regime conceptually depicted in Figure 10 holds, such transfer should not occur through advection alongside a front, but rather through diffusive transport across the 12°E–23°E domain. Moreover, the very existence of such interocean transport is uncertain, as the subtropical water present north of the SSTF in the Atlantic Ocean might be mostly entrained northward after being mixed east of ~12°E. Surface float trajectories in this region [*Piola et al.*, 1987] suggest such a behavior north of the SSTF latitude (~39°S). South of this latitude, the surface floats do proceed to the Indian Ocean but, from Figure 10, these reflect a transfer of original subantarctic water (not of subtropical water) even though this subantarctic water may gain some subtropical characteristics through mixing at 12°E–23°E, and eventually contribute to the water of intermediate properties in the AF-SSTF interval in the Indian Ocean.

[57] While Figure 10 suggests a weak interocean transfer of original Atlantic subtropical water at the upper levels (Central Water), the eastward flow might be more efficient at greater depths. *You et al.* [2003] found an eastward extending tongue of Antarctic Intermediate Water of Atlantic origin at 42°S–48°S south of Africa [*You et al.*, 2003, Figure 7], that is, just north of the time-averaged latitude of zero wind stress curl. Still deeper, diluted North Atlantic Deep Water is also known to flow eastward at such latitudes [*Arhan et al.*, 2003]. The SSTF disruption south of Africa therefore suggests an eastward limb of the supergyre that transports little original South Atlantic Central Water, and is enhanced at depth.

[58] This study confirmed a partial (and, from the above, possibly dominant at the upper levels) eastern closure of the South Atlantic subtropical gyre, related to the NSTF and Agulhas rings of the northern variety of *Dencausse et al.* [2010b]. Regarding the question of the subtropical gyre termination, we should also note the apparent important part played by the pool of cyclonic vorticity (the lee eddy of *Penven et al.* [2001]) often present between the Agulhas Bank and the Erica Seamount (Figures 3 and 7) in separating the South Atlantic and South Indian Ocean subtropical gyres. In the southern Indian Ocean, the upper water with intermediate properties observed in previous studies between the AF and SSTF is the likely result of mixing at longitudes 12°E–23°E, between subantarctic water and Central water. The erosion of Agulhas rings and Agulhas eddies observed as far south as 42°S–43°S might be important in modifying the original subantarctic water characteristics.

[59] The SSTF discontinuity south of Africa, finally, makes this region a favorable place for upper level exchanges between the subantarctic and subtropical domains. Such exchanges naturally occur at other longitudes through meandering and eddy shedding at the SSTF. As underlined above, the regime is different at 12°E–23°E, with the eddies originating from the Agulhas Current system, not the SSTF. The efficient role of Agulhas rings in carrying subantarctic water northward was pointed out in previous studies. The rings (from *Dencausse et al.*'s [2010b] southern route) and Agulhas eddies [*Lutjeharms and Valentine*, 1988] passing in the subantarctic zone at 12°E–23°E should similarly be important for a southward transfer of subtropical properties. Our results even suggest that their release of warm and salty water into the subantarctic zone might position the southern boundary of the south Indian Ocean subtropical domain a few degrees to the south of the AF, at the SSTF. If real, this process would constitute a strong interrelation between the Indo-Atlantic and subantarctic-subtropical exchanges south of Africa.

References

Arhan, M., H. Mercier, and J. R. E. Lutjeharms (1999), The disparate evolution of three Agulhas rings in the South Atlantic Ocean, *J. Geophys. Res.*, *104*, 20,987–21,005.

Arhan, M., H. Mercier, and Y.-H. Park (2003), On the deep water circulation of the eastern South Atlantic Ocean, *Deep Sea Res. Part I*, *50*, 889–916, doi:10.1016/S0967-0637(03)00072-4.

Belkin, I. M. (1993), Frontal structure of the South Atlantic (in Russian), in *Pelagic Ecosystems of the Southern Ocean*, edited by N. M. Voronina, pp. 40–53, Nauka, Moscow.

Belkin, I. M., and A. L. Gordon (1996), Southern Ocean fronts from the Greenwich meridian to Tasmania, *J. Geophys. Res.*, *101*, 3675–3696, doi:10.1029/95JC02750.

Boebel, O., J. Lutjeharms, C. Schmid, W. Zenk, T. Rossby, and C. Barron (2003a), The Cape Cauldron: A regime of turbulent inter-ocean exchange, *Deep Sea Res. Part II*, *50*, 57–86, doi:10.1016/S0967-0645 (02)00379-X.

Boebel, O., T. Roosby, J. Lutjeharms, W. Zenk, and C. Barron (2003b), Path and variability of the Agulhas Return Current, *Deep Sea Res. Part II*, *50*, 35–56, doi:10.1016/S0967-0645(02)00377-6.

Boudra, D. B., and E. P. Chassignet (1988), Dynamics of Agulhas retroflection and ring formation in a numerical model. Part I: The vorticity balance, *J. Phys. Oceanogr.*, *18*, 280–303, doi:10.1175/1520-0485 (1988)018<0280:DOARAR>2.0.CO;2.

Boudra, D. B., and W. P. M. de Ruijter (1986), The wind-driven circulation of the South Atlantic-Indian Ocean—Part II. Experiments using a multilayer numerical model, *Deep Sea Res.*, *33*, 447–482, doi:10.1016/0198-0149(86)90126-3.

Burls, N. J., and C. J. C. Reason (2006), Sea surface temperature fronts in the midlatitude South Atlantic revealed by using microwave satellite data, *J. Geophys. Res.*, *111*, C08001, doi:10.1029/2005JC003133.

Chassignet, E. P., and D. B. Boudra (1988), Dynamics of Agulhas retroflection and ring formation in a numerical model. Part II. Energetics and ring formation, *J. Phys. Oceanogr.*, *18*, 304–319, doi:10.1175/1520-0485(1988)018<0304:DOARAR>2.0.CO;2.

Deacon, G. E. R. (1982), Physical and biological zonation in the Southern Ocean, *Deep Sea Res.*, *29*, 1–15, doi:10.1016/0198-0149(82)90058-9.

Dencausse, G., M. Arhan, and S. Speich (2010a), Spatio-temporal characteristics of the Agulhas Current retroflection, *Deep Sea Res. Part I*, *57*, 1392–1405, doi:10.1016/j.dsr.2010.07.004.

Dencausse, G., M. Arhan, and S. Speich (2010b), Routes of Agulhas rings in the southeastern Cape Basin, *Deep Sea Res. Part I*, *57*, 1406–1421, doi:10.1016/j.dsr.2010.07.008.

de Ruijter, W. (1982), Asymptotic analysis of the Agulhas and Brazil Current systems, *J. Phys. Oceanogr.*, *12*, 361–373, doi:10.1175/1520-0485(1982)012<0361:AAOTAA>2.0.CO;2.

de Ruijter, W. P. M., and D. B. Boudra (1985), The wind-driven circulation in the South Atlantic-Indian Ocean—Part I. Numerical experiments in a one-layer model, *Deep Sea Res.*, *32*, 557–574, doi:10.1016/0198-0149 (85)90044-5.

de Ruijter, W. P. M., A. Biastoch, S. S. Drijfhout, J. R. E. Lutjeharms, R. P. Matano, T. Pichevin, P. J. van Leeuwen, and W. Weijer (1999), Indian-Atlantic interocean exchange: Dynamics, estimation and impact, *J. Geophys. Res.*, *104*, 20,885–20,910, doi:10.1029/1998JC900099.

Ducet, N., P. Y. Le Traon, and G. Reverdin (2000), Global high-resolution mapping of ocean circulation from TOPEX/Poseidon and ERS-1 and-2, *J. Geophys. Res.*, *105*, 19,477–19,498, doi:10.1029/2000JC900063.

Duncan, C. P. (1968), An eddy in the Subtropical Convergence southwest of South Africa, *J. Geophys. Res.*, *73*, 531–534, doi:10.1029/JB073i002p00531.

Gladyshev, S., M. Arhan, A. Sokov, and S. Speich (2008), A hydrographic section from South Africa to the southern limit of the Antarctic Circumpolar Current at the Greenwich meridian, *Deep Sea Res. Part I*, *55*, 1284–1303, doi:10.1016/j.dsr.2008.05.009.

Gordon, A. L., and K. T. Bosley (1991), Cyclonic gyre in the tropical South Atlantic, *Deep Sea Res.*, *38*, suppl., S323–S343.

Gordon, A. L., R. F. Weiss, W. M. Smethie Jr., and M. J. Warner (1992), Thermocline and intermediate water communication between the South Atlantic and Indian oceans, *J. Geophys. Res.*, *97*, 7223–7240, doi:10.1029/92JC00485.

Gründlingh, M. L. (1978), Drifts of satellite-tracked buoys in the southern Agulhas Current and Agulhas Return Current, *Deep Sea Res.*, *25*, 1209–1224, doi:10.1016/0146-6291(78)90014-0.

Holliday, N. P., and J. F. Read (1998), Surface oceanic fronts between Africa and Antarctica, *Deep Sea Res. Part I*, *45*, 217–238, doi:10.1016/S0967-0637(97)00081-2.

Le Traon, P. Y., F. Nadal, and N. Ducet (1998), An improved mapping method of multisatellite altimeter data, *J. Atmos. Oceanic Technol.*, *15*, 522–534, doi:10.1175/1520-0426(1998)015<0522:AIMMOM>2.0.CO;2.

Lutjeharms, J. R. E. (1985), Locations of frontal systems between Africa and Antarctica: Some preliminary results, *Deep Sea Res.*, *32*, 1499–1509, doi:10.1016/0198-0149(85)90100-1.

Lutjeharms, J. R. E. (2006), *The Agulhas Current*, 329 pp., Springer, Berlin.

Lutjeharms, J. R. E., and H. R. Valentine (1984), Southern Ocean thermal fronts south of Africa, *Deep Sea Res.*, *31*, 1461–1475, doi:10.1016/0198-0149(84)90082-7.

Lutjeharms, J. R. E., and H. R. Valentine (1988), Eddies at the Subtropical Convergence south of Africa, *J. Phys. Oceanogr.*, *18*, 761–774, doi:10.1175/1520-0485(1988)018<0761:EATSCS>2.0.CO;2.

Lutjeharms, J. R. E., and R. C. Van Ballegooyen (1988), The retroflection of the Agulhas Current, *J. Phys. Oceanogr.*, *18*, 1570–1583, doi:10.1175/1520-0485(1988)018<1570:TROTAC>2.0.CO;2.

Lutjeharms, J. R. E., O. Boebel, and H. T. Rossby (2003), Agulhas cyclones, *Deep-Sea Res. Part II*, *50*, 13–34, doi:10.1016/S0967-0645(02)00378-8.

Orsi, A. H., T. Whitworth, and W. D. Nowlin (1995), On the meridional extent and fronts of the Antarctic Circumpolar Current, *Deep Sea Res. Part I*, *42*, 641–673, doi:10.1016/0967-0637(95)00021-W.

Park, Y.-H., E. Charriaud, and P. Craneguy (2001), Fronts, transports, and Weddell gyre at 30°E between Africa and Antarctica, *J. Geophys. Res.*, *106*, 2857–2879, doi:10.1029/2000JC900087.

Penven, P., J. R. E. Lutjeharms, P. Marchesiello, C. Roy, and S. J. Weeks (2001), Generation of cyclonic eddies by the Agulhas Current in the lee of the Agulhas Bank, *Geophys. Res. Lett.*, *28*, 1055–1058, doi:10.1029/2000GL011760.

Peterson, R. G., and L. Stramma (1991), Upper-level circulation in the South Atlantic Ocean, *Prog. Oceanogr.*, *26*, 1–73, doi:10.1016/0079-6611(91)90006-8.

Piola, A. R., H. A. Figueroa, and A. A. Bianchi (1987), Some aspects of the surface circulation south of 20°S revealed by First GARP Global Experiment drifters, *J. Geophys. Res.*, *92*, 5101–5114, doi:10.1029/JC092iC05p05101.

Read, J. F., and R. T. Pollard (1993), Structure and transport of the Antarctic Circumpolar Current and Agulhas Return Current at 40°E, *J. Geophys. Res.*, *98*, 12,281–12,295, doi:10.1029/93JC00436.

Rio, M.-H., and F. Hernandez (2004), A mean dynamic topography computed over the world ocean from altimetry, in situ measurements, and a geoid model, *J. Geophys. Res.*, *109*, C12032, doi:10.1029/2003JC002226.

Rio, M.-H., P. Schaeffer, J.-M. Lemoine, and F. Hernandez (2005), Estimation of the ocean Mean Dynamic Topography through the combination of altimetric data, in-situ measurements and GRACE geoid: From global to regional studies, paper presented at Geoid and Ocean Circulation in the North Atlantic International Workshop, Eur. Space Agency, Luxembourg.

Smythe-Wright, D., P. Chapman, C. Duncombe Rae, L. V. Shannon, and S. M. Boswell (1998), Characteristics of the South Atlantic subtropical frontal zone between 15°W and 5°E, *Deep Sea Res. Part I*, *45*, 167–192, doi:10.1016/S0967-0637(97)00068-X.

Sokolov, S., and S. R. Rintoul (2009), Circumpolar structure and distribution of the Antarctic Circumpolar Current fronts: 1. Mean circumpolar paths, *J. Geophys. Res.*, *114*, C11018, doi:10.1029/2008JC005108.

Stramma, L., and J. R. L. Lutjeharms (1997), The flow field of the subtropical gyre of the South Indian Ocean, *J. Geophys. Res.*, *102*, 5513–5530, doi:10.1029/96JC03455.

Stramma, L., and R. G. Peterson (1990), The South Atlantic Current, *J. Phys. Oceanogr.*, *20*, 846–859, doi:10.1175/1520-0485(1990) 020<0846:TSAC>2.0.CO;2.

Swart, S., and S. Speich (2010), An altimetry-based gravest empirical mode south of Africa: 2. Dynamic nature of the Antarctic Circumpolar fronts, *J. Geophys. Res.*, *115*, C03003, doi:10.1029/2009JC005300.

Whitworth, T., and W. D. Nowlin (1987), Water masses and currents of the Southern Ocean at the Greenwich meridian, *J. Geophys. Res.*, *92*, 6462–6476, doi:10.1029/JC092iC06p06462.

You, Y., J. R. E. Lutjeharms, O. Boebel, and W. P. M. de Ruijter (2003), Quantification of the inter-ocean exchange of intermediate water masses around southern Africa, *Deep Sea Res. Part II*, *50*, 197–228, doi:10.1016/S0967-0645(02)00384-3.

M. Arhan and S. Speich, Laboratoire de Physique des Océans, CNRS/IFREMER/IRD/UBO, BP 70, F-29280 Plouzané, France.

G. Dencausse, Laboratoire d'Etudes en Géophysique et Océanographie Spatiale, LEGOS/OMP, 14 Ave. Edouard Belin, F-31400 Toulouse, France. (guillaume.dencausse@legos.obs-mip.fr)